

1 **A new daily observational record from Grytviken, South Georgia: exploring 20th**
2 **century extremes in the South Atlantic**

3

4 Zoë Thomas^{1,2*}, Chris Turney^{1,2}, Rob Allan³, Steve Colwell⁴, Gail Kelly³, David Lister⁵,
5 Philip Jones^{5,6}, Mark Beswick⁷, Lisa Alexander^{2,8}, Tanya Lippmann⁹, Nicholas Herold^{2,8},
6 and Richard Jones¹⁰

7

8 ¹Palaeontology, Geobiology and Earth Archives Research Centre, School of Biological,
9 Earth And Environmental Science, University of New South Wales, Sydney, Australia

10 ²Climate Change Research Centre, School of Biological, Earth And Environmental
11 Science, University of New South Wales, Sydney, Australia

12 ³Met Office Hadley Centre/ACRE, Exeter, UK

13 ⁴British Antarctic Survey, Cambridge, UK

14 ⁵Climatic Research Unit, School of Environmental Sciences, University of East Anglia,
15 Norwich, UK

16 ⁶Center of Excellence for Climate Change Research, Department of Meteorology, King
17 Abdulaziz University, Jeddah, 21589, Saudi Arabia

18 ⁷National Library & Archive, Met Office, Exeter, UK

19 ⁸ARC Centre of Excellence for Climate System Science, University of New South Wales,
20 Sydney, Australia

21 ⁹Faculty of Earth and Life Sciences, Vrije Universiteit Amsterdam, Netherlands

22 ¹⁰Department of Geography, Exeter University, Devon, EX4 4RJ, UK

23

24 *z.thomas@unsw.edu.au

25

26 **Abstract**

27 Although recent work has highlighted a host of significant late 20th century
28 environmental changes across the mid to high latitudes of the Southern Hemisphere, the
29 sparse nature of observational records limits our ability to place these changes in the
30 context of long-term (multi-decadal and centennial) variability. As a result, investigating
31 the impact of anthropogenic forcing on climate modes of variability and ecosystems is
32 particularly challenging, though historical records from sub-Antarctic islands offer the
33 potential to develop highly resolved records of change. In 1905, a whaling and
34 meteorological station was established at Grytviken on Sub-Antarctic South Georgia in
35 the South Atlantic (54°S, 36°W) providing near-continuous daily observations through
36 to present day. Here we report this new, previously unpublished, daily observational
37 record from Grytviken for temperature and precipitation, which we compare to different
38 datasets (including Twentieth Century Reanalysis; 20CR version 2c). We find a
39 significant trend towards increasingly warmer daytime extremes commencing from the
40 mid-20th century accompanied by warmer night-time temperatures, with an average
41 rate of temperature rise of 0.13°C per decade over the period 1907-2016 ($p < 0.0001$).
42 Analysis of these data, and reanalysis products, suggest a realignment of synoptic
43 conditions across the mid to high-latitudes since the mid-20th century, characterised by
44 stronger westerly airflow linked to warm foehn winds across South Georgia. These rapid
45 rates of warming have negative implications for biodiversity levels and the continued
46 survival of some marine biota across the region.

47

48 **1. Introduction**

49

50 Climate changes in the mid to high latitudes of the Southern Hemisphere have exhibited
51 extreme and regionally asymmetric trends in temperature and precipitation over the
52 last half century, with warming particularly marked over the Antarctic Peninsula and
53 South Atlantic during recent decades (Turner et al. 2005; Abram et al. 2014; Richard et
54 al. 2013; Turney et al. 2016a; Jones et al. 2016a). However, due to the sparse
55 distribution and temporal limitations of instrumental records, the long-term evolution
56 of climatically sensitive high latitude regions of the Southern Hemisphere, especially
57 prior to the 1950s, remains elusive. Sub-Antarctic islands are particularly important in
58 this regard, straddling major ocean and atmospheric boundaries and offering the
59 potential to develop highly resolved records of change. The ecosystems that inhabit
60 these islands are of global importance, with high biological diversity and productivity,
61 but appear to be increasingly vulnerable to late twentieth century change (Boyd et al.
62 2014; Constable et al. 2014; Trathan et al. 2012; Turney et al. 2017). Although invariably
63 remote, numerous whaling stations were established across the Southern Ocean islands
64 in the late 19th and early 20th century, where in some locations, daily weather
65 observations were meticulously recorded. Although South Georgia lies in a strategic
66 location for understanding Southern Ocean atmosphere-ocean dynamics, only a monthly
67 resolved dataset has until now been available. These historical data provide key records
68 for expanding the observational network, allowing a better characterisation of climate
69 variability across southern latitudes.

70

71 South Georgia is a relatively small, mountainous and heavily glaciated Sub-Antarctic
72 island (~3500 km²) located approximately 1500 km northeast of the Antarctic

73 Peninsula (Figure 1). It has experienced substantial glacier retreat during the second
74 half of the 20th century, with particularly dramatic losses during the first decade of the
75 21st century (Cook et al. 2010; Gordon et al. 2008). While the precise drivers of this
76 glacier retreat remain unclear, due to the large potential and diverse impacts of this
77 retreat on the terrestrial and marine biota, understanding these drivers of change is
78 crucial (Cook et al. 2010; Murphy et al. 2007). Fortunately in this regard, (though
79 resulting in devastating local impact on fauna) the island was home to numerous
80 whaling stations after 1905, of which the station at Grytviken, the longest operating
81 whaling station on the island, provides the longest and most complete meteorological
82 records. While monthly climate statistics from Sub-Antarctic South Georgia are
83 currently available in the public domain, disentangling changes in extremes requires
84 daily-resolved data. A coordinated effort was therefore undertaken to locate and
85 transcribe the records from Grytviken, to improve our understanding of South Atlantic
86 climate change through the 20th century.

87

88

89 **2. Data and Methods**

90

91 The establishment of a whaling and meteorological station at Grytviken, South Georgia
92 (also known as Cumberland Bay or King Edward Point), in 1905 allowed the creation of
93 one of the longest observational records from the high latitudes of the Southern
94 Hemisphere. Between 1905 and 1969 the occupying Norwegian-Argentine whaling
95 station (Compania Argentina de Pesca) took meteorological readings. Following this, the
96 British Falkland Island Dependencies Survey (and later British Antarctic Survey) took
97 ownership of the station until the outbreak of the South Atlantic Conflict in April 1982. A

98 small British Military garrison reoccupied the station weeks later, where they remained
99 until March 2001. Near-continuous measurements were taken from 1905 to 1982, and
100 although it is believed that the occupying military did take meteorological readings,
101 uncertainty over the station layout and the location of the data has unfortunately
102 resulted in an eighteen-year gap in the record. Monthly data from 1984-1988 are
103 available from BAS, but so far no daily data or metadata have been identified. We
104 therefore exclude these data from our analyses, and highlight these unverified data
105 where shown. The British Antarctic Survey returned to the island in March 2001 and set
106 up an automatic weather station (AWS), providing continuous measurements to the
107 present day.

108

109 The meteorological station of Grytviken is located on the north coast of South Georgia
110 (World Meteorological Organization station number: 88903; 54°16'59"S, 36°30'0"W).
111 The weather station is located at an altitude of 2.2 m above mean sea level. The data
112 from the early Norwegian-Argentine occupation from 1905 to 1962 are archived at the
113 Met Office archives in Exeter, UK, and from 1963-1982 at the British Antarctic Survey
114 Archives in Cambridge, UK. Data from the automated weather station present since
115 2001 can be accessed via [https://legacy.bas.ac.uk/cgi-bin/metdb-form-](https://legacy.bas.ac.uk/cgi-bin/metdb-form-2.pl?tabletouse=U_MET.GRYTVIKEN_AWS&complex=1&idmask=.....&acct=u_met&pass=)
116 [2.pl?tabletouse=U_MET.GRYTVIKEN_AWS&complex=1&idmask=.....&acct=u_met&pass=](https://legacy.bas.ac.uk/cgi-bin/metdb-form-2.pl?tabletouse=U_MET.GRYTVIKEN_AWS&complex=1&idmask=.....&acct=u_met&pass=)
117 weather. The data elements transcribed were daily maximum temperatures (TX), daily
118 minimum temperatures (TN) and daily precipitation totals (PREC).

119

120 Metadata for the meteorological station are detailed, including height above ground,
121 particulars of the instruments, and dates and details of any station/instrument location
122 changes. Importantly, this metadata allows us to cross-check with our homogeneity tests

123 to confirm the integrity of the record. For instance, when the station changed hands
124 from Argentine to British control, metadata from the station reads: "The former station
125 closed in 1948 and was replaced by King Edward Point, the two sites should be
126 compatible. Reliability: compared with 888900 [Stanley] and 879680 [OrCADAS] for the
127 years 1923-1980 and 1905-1980." It was also established from the metadata that
128 temperature data from January 1905 to June 1907 should be discounted due to faulty
129 exposure of the thermometers, which were affected by solar radiation, providing
130 erroneously high readings. Although the thermometer screen was reported to have
131 moved in January 1978, there is no evidence that this created a difference in the
132 temperature readings. However, there is no known metadata available when the station
133 was under military control, except that the thermometer screen was moved. The Milos
134 500 AWS was installed in March 2001, providing hourly readings, and was replaced by a
135 Milos 530 AWS in 2006, which records one-minute observations. Both AWS used a
136 platinum resistance thermometer probe, with an accuracy of $\pm 0.2^{\circ}\text{C}$. In terms of
137 precipitation data, up to 1982 measurements were taken with a Snowdon rain gauge,
138 which can under-read in snow conditions as the wind can blow some of the snow over
139 the top of the gauge (Goodison et al. 1998). The data since 2010 have been collected
140 using a Laser Precipitation Monitor, which is thought to be more accurate. However,
141 since there is no overlap between the two instrumentation methods, there is no way to
142 assess how different the totals are, thus long-term trends that include data using both
143 instruments should be interpreted with extreme caution. Homogeneity tests were
144 undertaken to detect and adjust for sudden step changes present in the time series for
145 reasons other than climatic changes (such as instrument change) using the software
146 package RHTestsv4 (Wang 2008a,b; Wang and Feng 2013), and found no significant
147 inhomogeneities in the daily precipitation, maximum or minimum temperature data.

148

149 Basic quality controls have been undertaken for all series following the procedures
150 outlined in Alexander et al. (2006), and where necessary, unreliable data removed.
151 Missing data criteria were adapted from Zhang et al. (2011) and applied as follows:
152 monthly indices were calculated if no more than 3 days are missing in a month, seasonal
153 indices were calculated if no more than 6 days missing in the three month period (and
154 no more than four days missing per month), while annual values were calculated if no
155 more than 15 days are missing in a year and no single month is missing. In addition to
156 the missing data between March 1982 and March 2001, there are several other gaps in
157 the observations associated with observer illness or instrumentation problems affecting
158 the following periods: October 1910 to May 1911; January 1919 to April 1920; March to
159 April 1928; and May 1946 to December 1949. After the AWS was installed in 2001, there
160 were occasional issues with the automatic instrumentation and/or computer that could
161 take several days to resolve (this was particularly acute during 2007). In addition, the
162 data were removed between September 1968 and December 1969, owing to suspect
163 diurnal temperature range and unusually high precipitation values. It is worth noting
164 that while rarely transcribed, log books often have valuable qualitative data in addition
165 to the quantitative data recorded. Following identification of potentially spurious
166 value(s), we looked at the original photographs taken to help identify any transcription
167 errors, and if there were any qualitative comments made that could help to corroborate
168 the values. For example, in August 1939, the mean monthly temperature is one degree
169 lower than the next lowest monthly temperature. The logbook was consulted, and
170 determined that there were no transcription errors. Instead, comments in the
171 'observations' section had several phrases indicating particularly cold conditions: "*muy*
172 *frio*" (very cold), "*ventisca dia y noche*" (blizzard day and night), "*viento fuerte*" (strong

173 wind) and “*temperatura muy baja*” (temperature very low). Qualitative data such as
174 these can be valuable sources of extra quality assurance.

175

176 The data were analysed using R-based CLIMPACT software package (Alexander and
177 Herold 2015) to calculate selected extreme climate indices (Zhang et al. 2011). We use
178 daily minimum (TN) and maximum (TX) temperature as well as daily precipitation in
179 this assessment. We use percentile-based threshold levels using 1950-1980 as our
180 baseline, including the 90th percentile of the daily minimum (TN90p) and maximum
181 (TX90p) temperature to measure changes in moderate extremes. We used a generalized
182 least squares approach, fit by maximizing the restricted log-likelihood (REML) with
183 autoregressive (AR) errors, to estimate the slope term of an assumed linear trend. We
184 utilised the Akaike information criterion (AIC) to compare different models and chose
185 an autoregressive model of order AR(1), which was determined to successfully remove
186 autocorrelation of the residuals. The trends are reported as °C of warming per decade
187 or precipitation sum (mm) increase per decade calculated for each period, with the
188 associated standard error and *p* value. To further explore the atmospheric drivers of
189 observed climate changes we also use the ACRE-facilitated NOAA-CIRES Twentieth
190 Century Reanalysis Project (20CR version 2c) (Compo et al. 2011; Giese et al. 2016). The
191 data will be publically accessible via the ISTI (International Surface Temperature
192 Initiative; <http://www.surface temperatures.org/>) and the GPCC (Global Precipitation
193 Climatology Centre; <https://www.esrl.noaa.gov/psd/data/gridded/data.gpcc.html>).

194

195

196 **3. Results**

197

198 A warming trend over the 20th century is observed in mean monthly temperature at
199 Grytviken from daily data (calculated as the average of TX and TN) (Figure 2), with an
200 average rate of temperature rise of 0.14°C per decade over the period 1907-2016
201 ($p < 0.0001$; Table 1), calculated from the annual mean. However, more detailed analysis
202 of this rate of increase shows a slight decrease in temperatures over the first two
203 decades of the record at South Georgia, before the warming trend was established.
204 When splitting the record approximately in half (1906-1950, and 1951-2016), there is
205 no significant trend identified in the early half of the twentieth century, but a strong
206 trend in the latter half, peaking at 0.22°C per decade ($p < 0.0002$; Table 1). Importantly,
207 however, the rate of warming is not constant year round. When seasonal trends are
208 investigated, the largest warming trend occurs during the austral spring and summer
209 months (Table 1).

210

211 To determine whether the AWS station is producing temperatures that would bias the
212 trends, we compare the observations from South Georgia to the Twentieth Century
213 Reanalysis (20CR v2c) (Figure 2B). We observe a close correspondence between the two
214 time series (Pearson product-moment correlation of 0.648, $p = 3.099E-09$), though it is
215 important to note that due to South Georgia's small size, the reanalysis assigns it as an
216 ocean grid box rather than a land box, which helps to explain the lower variability in the
217 reanalysis time series. The decadal rates of change over different time periods for the
218 reanalysis data are reported in Table 2. These show coherence to the observational
219 trends, in all periods, suggesting that the data from the AWS have not biased the linear
220 trend since 1950.

221

222 To investigate the distribution of temperatures across the seasons more fully, we
223 explored the probability distribution functions for daily seasonal temperatures at South
224 Georgia over each 20-year period since 1907 (Figure 3). Although the shape of the
225 distributions remains largely unchanged (with only a slight shift to a more positively
226 skewed distribution between the first and second half of the 20th century in all seasons),
227 TX and TN appear to have shifted to the right through the 20th century. Most notably,
228 the overall distribution in TX and TN appears to have remained broadly the same across
229 the period 1907-1966 but subsequent bi-decadal averages show a mostly uniform shift
230 to higher temperatures, most notably during the austral spring and summer. This shift
231 implies that there was a change in the frequency of occurrence of cold and warm
232 extremes across the mid-twentieth century, with more frequent warm extremes and less
233 frequent cold extremes experienced over recent decades compared to the beginning of
234 the 20th century.

235

236 Since some weather extremes are predicted to become more frequent due to
237 anthropogenic influences on climate (Field et al. 2012), past extremes can provide a
238 baseline for comparing modern extremes. However, since extremes are inherently rare
239 events, we look at 'moderate' extreme indices, defined as those that occur several times
240 per year, rather than rarer events whose statistics would be harder to robustly
241 characterise (Sardeshmukh et al. 2015; Zhang et al. 2011). To further explore the
242 changes of warm and cool extremes during the summer and winter, we therefore
243 analysed the change in the frequency of occurrence of temperatures exceeding the 90th
244 percentile (TX90p and TN10p) using the period 1950-1980 as a baseline. Here we
245 observe an increase in the frequency of moderate warm extremes during the austral
246 summer (December-February) and a decrease in the occurrence of moderate cool

247 extremes during winter (June-August) (Figure 4). The mean minimum temperature in
248 DJF increased from 1.05°C in 1907-1926 to 1.61°C in 1947-1966 and to 2.47°C in 2001-
249 2016, with their standard deviations at 2.14, 1.96 and 2.30 respectively. A similar
250 pattern was found for the mean maximum temperature in DJF, increasing by a total of
251 1.5°C over the same period.

252

253 Analysis of the annual precipitation total (using totals with <6 missing observations per
254 year) shows a strong increasing trend through the 20th century (Figure 5), representing
255 an average increase of approximately 40 mm per year (though this is superimposed on a
256 highly variable time series). A marked shift in the amount of precipitation is observed
257 from the most recent period (2010-2016), but due to possible inhomogeneities caused
258 by instrument changes from 2010 (though none were detected in our tests, there is a 28
259 year gap between the two types of instrument), it remains unclear how significant this
260 is. It is possible that the increasing precipitation trend described above may have
261 resulted in more precipitation falling as rain, rather than snow, which is better recorded
262 (Forland and Hanssen-bauer 2000; Hanssen-Bauer 2002; Førland and Hanssen-Bauer
263 2001). It is noted, however, that even omitting the 2010-2016 precipitation totals still
264 results in a significant increasing trend in annual precipitation sum (Figure 5 and Table
265 2). To understand the seasonal variation in rainfall, we divided the data into seasons
266 (December-February (DJF), March-May (MAM), June-August (JJA) and September-
267 November (SON); Figure 6), where there is a clear bias towards higher precipitation in
268 autumn and winter. In addition, the trajectory of the locally weighted scatterplot
269 smoothing lines indicates a greater rate of increase in precipitation in these seasons
270 (and with lower totals, but similar rates of increase in SON), suggesting that whatever
271 mechanism is driving the increase in precipitation, it dominates in autumn and winter.

272

273

274 **4. Discussion**

275

276 The warming trends observed at Grytviken, South Georgia, are comparable to the trends
277 from nearby Orcadas station on Laurie Island on the eastern side of the Antarctic
278 Peninsula (Zazulie et al. 2010). The total amount of annual mean warming at Grytviken
279 between 1907 and 2016 is 1.52°C ($2.32\text{E-}06$; Table 1) equivalent to an average
280 rate of 0.14°C per decade, comparable to the 0.2°C per decade observed at Laurie Island
281 (1903-2008) (Zazulie et al. 2010). A strong seasonal component is identified in the
282 South Georgia dataset, however, with the austral summer months contributing most to
283 the annual trend, particularly during the second half of the 20th century (Table 1) (1951-
284 2017; 0.21°C per decade, $p=0.0002$). Similar seasonal differences in trends are also
285 observed at Orcadas, with the rate of summer warming in the latter half of the 21st
286 century double that of the early 21st century (Zazulie et al. 2010). Compared to the
287 Falkland Islands, the linear trend of the temperature series from 1920-2010 is 0.05°C
288 per decade ($p=0.002$) (Lister and Jones 2014; Jones et al. 2016b), which is substantially
289 lower than South Georgia.

290

291 It is important to note here that many warm extremes on South Georgia relate to foehn
292 winds, which are defined as strong, warm, dry winds that descend from mountains
293 (Skansi et al. 2017). Much of South Georgia's climate is strongly modified by the steep
294 orography, with a high mountain chain >2000 metres above sea level down the spine of
295 the island. Located within the belt of the westerly winds, the island acts as a natural
296 barrier to the prevailing airflow. Strong prevailing airflow over a topographic obstacle

297 results in an adiabatic cooling of the rising air at the moist adiabatic lapse rate, causing
298 latent heat to be released and precipitation to occur, decreasing the humidity of the
299 advected air. As the parcel then starts to descend down the leeward slope, it warms at
300 the faster dry adiabatic lapse rate, resulting in a temperature and humidity gradient
301 between the windward and leeward side of the topographic barrier at the same
302 elevation (Elvidge and Renfrew 2016; Skansi et al. 2017). Foehn warming can also take
303 place without precipitation, where warming on the leeside of a topographic barrier can
304 be generated by the descent of warmer air sources above it caused by blocked flow
305 (Elvidge and Renfrew 2016). These foehn winds have been shown to be frequent;
306 occurring approximately every 4 days, and capable of warming the daily mean
307 temperature by up to 20°C, with a mean increase in temperature across all events of
308 ~10°C (as measured between 2003-2013) (Bannister 2015). While wind speed and
309 direction was recorded at South Georgia since 1905, this has not yet been transcribed
310 (in part due to the notorious unreliability of historical observational wind data), limiting
311 our understanding of foehn winds during the 20th century. However, wind speed and
312 direction have been measured with the AWS on South Georgia since installation in 2001,
313 though unfortunately, due to local topographic modification (e.g. wind channelling), the
314 recorded wind direction at King Edward Point is not indicative of the synoptic wind
315 pattern. Instead, in Bannister et al. (2015), ERA-Interim reanalysis was used to illustrate
316 synoptic conditions during foehn events, and showed a well-defined ridge of high
317 pressure, roughly centred just north of South Georgia, during strong foehn conditions, a
318 feature that is absent in the climatological mean.

319

320 There are several important modes of variability that affect climate and weather in the
321 high latitudes of the South Atlantic. One mode of variability is the Pacific-South

322 American (PSA) teleconnection pattern, through which the El Niño-Southern Oscillation
323 (ENSO) signal propagates into high southern latitudes during the austral
324 spring/summer (Mo and Higgins 1998; Ding et al. 2012), causing strong northerlies to
325 advect warm maritime air from the South Pacific towards South Georgia. Related to this,
326 an increase in Rossby wave penetration thought to be linked to tropical Pacific
327 temperatures has been suggested to play a potential role in the evolution of Antarctic
328 climate since the mid 20th century (Fogt et al. 2011; Ding et al. 2012; Turney et al. 2017,
329 2016a).

330

331 The major mode of variability in atmospheric circulation in the high southern latitudes,
332 however, is the Southern Annular Mode (SAM); a circumpolar pattern of pressure
333 gradients defined as the zonal mean atmospheric pressure difference between 40°S and
334 65°S (Marshall 2003; Thompson et al. 2011). The multi-decadal trend to a more positive
335 SAM since the mid-20th century (Abram et al. 2014) is manifested by a strengthening
336 and southward shift of westerly airflow over the Southern Ocean (Visbeck 2009;
337 Marshall 2003; Thompson et al. 2011). Although the increase in the SAM index has
338 occurred in all seasons, the most pronounced trend is observed over the summer-
339 autumn (Marshall 2003). The impact of SAM may have been amplified as a result of the
340 spring Antarctic ozone hole which established in the late 1970s and exerts its greatest
341 effect on climate and circulation patterns during the summer (Thompson and Solomon
342 2002; Zazulie et al. 2010). However, the warming trends observed from South Georgia
343 start before this time, suggesting that ozone cannot be the sole driver of the warming
344 trends observed. Indeed, although of a smaller magnitude, warming is also observed in
345 the winter months.

346

347 The precipitation trends observed from South Georgia differ in two main aspects to the
348 temperature trends: firstly, that increasing precipitation appears to commence from the
349 beginning of the 20th century, and secondly, the increases appear to occur mainly over
350 the autumn and winter months. The difference in temperature and precipitation trends
351 (both the timing of the changes and the seasonality) suggests different climate drivers.
352 Several other records from nearby meteorological stations also observe a long term
353 increase in precipitation, including the annual precipitation recorded on the Falklands
354 Islands (Lister and Jones 2014; Jones et al. 2016b) and greatly increased snow
355 accumulation on the Antarctic Peninsula (Thomas et al. 2008). To elucidate the
356 dominant atmospheric circulation that might explain the observed climate and weather
357 extremes over South Georgia, we utilised the Twentieth Century Reanalysis, 20CR
358 version 2c (Compo et al. 2011) (Figure 7 and 8).

359
360 We investigate the total precipitation sum in autumn and winter (March-August) and
361 correlate to the 850hPa geopotential height and the 850hPa meridional wind over the
362 period 1905-1983 (the data gap between 1983 and 2010 unfortunately prevents
363 analysis in recent decades). We observe a correlation between low pressure over South
364 America and precipitation at South Georgia, allowing the delivery of moisture via
365 northerly and easterly airflow over South Georgia (Figure 7). Although the Amundsen
366 Sea Low is generally associated with quasi-stationary low pressure systems (Clem and
367 Fogt 2015), when large seasonal variability across the region allows a low pressure
368 system to develop over South America, our analysis shows more rainfall is delivered via
369 meridional airflow over South Georgia. The increasing trends in rainfall from the South
370 Georgia climate records are in general agreement with Turney et al. (2016a) who
371 reported higher rainfall over the Falkland Islands from the 1940s (as reported in Lister

372 and Jones (2014)), consistent with a lower mean sea level pressure in the South Atlantic
373 and higher pressure in the Amundsen Sea Low, leading to an unprecedented increase in
374 growth of peat sequences relative to the last 6000 years.

375

376 However, while the above mechanisms dominate in winter, causing enhanced
377 precipitation over South Georgia, there is a seasonal change in the configuration of the
378 synoptic conditions, consistent with the summer impact of SAM. We therefore
379 investigate the summer months (December-February) in mean monthly temperature,
380 correlating with the 850hPa geopotential height, and the 850hPa zonal wind to
381 understand the mechanisms of synoptic change. We split our data into an 'early' period
382 (1905-1950) and a 'late' period (1950-2016). Our analysis finds a strengthening
383 correlation between temperature and high-latitude zonal airflow over the 20th century,
384 resulting from a southwards shift in the circumpolar trough during the summer (Figure
385 8). Based on these results, we investigate the time series from the 20th Century
386 Reanalysis of the 850 hPa zonal wind over South Georgia, averaged over December-
387 February (Figure 9). We find a significant ($p < 0.036$) increasing trend in the zonal wind.
388 While there is no doubt that further work is needed to increase the density of early
389 observations in reanalysis products (such as the data reported in this paper), the
390 changing synoptic conditions that are produced are generally consistent with both
391 independent climate proxy data (Turney et al. 2016b; Amesbury et al. 2017) and
392 observations. These changes in the synoptic weather regimes give rise to surface
393 warming over South Georgia, through the relationship with the foehn effect. Although
394 the link between increasing westerly winds and warming over South Georgia may at
395 first seem counterintuitive, there is a demonstrated link between the strength of the
396 westerly winds and the occurrence and magnitude of foehn winds (Bannister and King

397 2015; Bannister 2015). If the strength of the winds is sufficiently high, downslope winds
398 develop on the (north-eastern) leeward side of the island, causing substantial temperature
399 increases as the descending air warms adiabatically. Regardless of the precise
400 mechanism of the generation of the foehn winds, the relationship between the positive
401 trend in SAM from the 1960s (Jones et al. 2009), enhancing westerly airflow over the
402 island, and the increased frequency and magnitude of foehn winds, helps to explain the
403 tendency for the high rate of summer warming and increasing frequency of warm
404 extremes that we observe in South Georgia over the past century.

405

406

407 **5. Wider Implications**

408

409 Changes to the climatic and environmental constraints that shape the current biological
410 diversity constitute the dominant threat to the island of South Georgia. Contemporary
411 glacier retreat resulted in the increased threat of invasive rat species from areas that
412 were previously isolated due to ice barriers (Cook et al. 2010). However, while a recent
413 program to eradicate rats was successfully implemented (Martin and Richardson 2017),
414 further biological invasions and colonisation of alien species will likely continue with the
415 current rate and direction of regional climate change. The South Georgian shelf is the
416 most speciose region of the Southern Ocean reported to date (Hogg et al. 2011), with a
417 cumulative dominance of endemic and range-edge species, many of which, such as
418 Antarctic krill *Euphausia superba*, show declining habitat suitability with warming
419 temperatures (Whitehouse et al. 2008). This in turn has negative impacts on the
420 breeding success of krill-dependent penguins and seals (Murphy et al. 2007). Critical to
421 this is the link between synoptic-scale and mesoscale meteorological processes. The

422 data presented here underscore the importance of the rescue of historical, daily-
423 resolved data from these remote islands to disentangle seasonal and extreme changes
424 and demonstrate a link between increasing temperature trends and atmospheric
425 circulation dominated by stronger westerly airflow, resulting in significant foehn-
426 related warming.

427

428

429 **Acknowledgments**

430 This work was supported by the Australian Research Council (FL100100195). This work
431 is part of the Atmospheric Circulation Reconstructions over the Earth (ACRE) initiative,
432 and Prof. Rob Allan is supported by funding from the Joint BEIS/Defra Met Office Hadley
433 Centre Climate Programme (GA01101). He also acknowledges the University of
434 Southern Queensland, Toowoomba, Australia, where he is an Adjunct Professor. Support
435 for the Twentieth Century Reanalysis Project version 2c dataset is provided by the U.S.
436 Department of Energy, Office of Science Biological and Environmental Research (BER),
437 and by the National Oceanic and Atmospheric Administration Climate Program Office.
438 We thank Gil Compo for valuable comments on the manuscript.

439

440

441 **References**

442 Abram, N. J., R. Mulvaney, F. Vimeux, S. J. Phipps, J. Turner, and M. H. England, 2014:
443 Evolution of the Southern Annular Mode during the past millennium. *Nat. Clim.*
444 *Chang.*, **4**, 1–6, doi:10.1038/NCLIMATE2235.

445 Alexander, L., and N. Herold, 2015: ClimPACTv2: indices and software. Technical report
446 of the World Meteorological Organisation Commission for climatology expert team

447 on sector-specific climate indices. World Meteorological Organisation.
448 <https://github.com/ARCCSS-extremes/climpact2/blob/mas>.

449 Alexander, L. V., and Coauthors, 2006: Global observed changes in daily climate
450 extremes of temperature and precipitation. *J. Geophys. Res. Atmos.*, **111**, 1–22,
451 doi:10.1029/2005JD006290.

452 Amesbury, M. J., T. P. Roland, J. Royles, D. A. Hodgson, P. Convey, H. Griffiths, and D. J.
453 Charman, 2017: Widespread Biological Response to Rapid Warming on the
454 Antarctic Peninsula. *Curr. Biol.*, **27**, 1616–1622.e2, doi:10.1016/j.cub.2017.04.034.
455 <http://dx.doi.org/10.1016/j.cub.2017.04.034>.

456 Bannister, D., 2015: Fohn winds on South Georgia and their impact on regional climate.
457 University of East Anglia, .

458 —, and J. King, 2015: Föhn winds on South Georgia and their impact on regional
459 climate. *Weather*, **70**, 324–329, doi:10.1002/wea.2587.

460 Boyd, P. W., S. T. Lennartz, D. M. Glover, and S. C. Doney, 2014: Biological ramifications of
461 climate-change-mediated oceanic multi-stressors. *Nat. Clim. Chang.*, **5**, 71–79,
462 doi:10.1038/nclimate2441.

463 Clem, K. R., and R. L. Fogt, 2015: South Pacific circulation changes and their connection
464 to the tropics and regional Antarctic warming in austral spring, 1979–2012. *J.*
465 *Geophys. Res. Atmos.*, **120**, 2773–2792, doi:10.1002/2014JD022940.Received.

466 Compo, G. P., and Coauthors, 2011: The Twentieth Century Reanalysis Project. *Q. J. R.*
467 *Meteorol. Soc.*, **137**, 1–28, doi:10.1002/qj.776.

468 Constable, A. J., and Coauthors, 2014: Climate change and Southern Ocean ecosystems I:
469 How changes in physical habitats directly affect marine biota. *Glob. Chang. Biol.*, **20**,
470 3004–3025, doi:10.1111/gcb.12623.

471 Cook, a J., S. Poncet, a P. R. Cooper, D. J. Herbert, and D. Christie, 2010: Glacier retreat on

472 South Georgia and implications for the spread of rats. *Antarct. Sci.*, **22**, 255–263,
473 doi:10.1017/s0954102010000064.

474 Ding, Q., E. J. Steig, D. S. Battisti, and J. M. Wallace, 2012: Influence of the tropics on the
475 southern annular mode. *J. Clim.*, **25**, 6330–6348, doi:10.1175/JCLI-D-11-00523.1.

476 Elvidge, A. D., and I. A. Renfrew, 2016: The causes of foehn warming in the lee of
477 mountains. *Bull. Am. Meteorol. Soc.*, **97**, 455–466, doi:10.1175/BAMS-D-14-00194.1.

478 Field, C. B., and Coauthors, 2012: *Managing the Risks of Extreme Events and Disasters to*
479 *Advance Climate Change Adaptation. A Special Report of Working Groups I and II of*
480 *the Intergovernmental Panel on Climate Change*. Cambridge University Press,
481 Cambridge, United Kingdom and New York, NY, USA, 582 pp.

482 Fogt, R. L., D. H. Bromwich, and K. M. Hines, 2011: Understanding the SAM influence on
483 the South Pacific ENSO teleconnection. *Clim. Dyn.*, **36**, 1555–1576,
484 doi:10.1007/s00382-010-0905-0.

485 Forland, E. J., and I. Hanssen-bauer, 2000: Increased precipitation in the Norwegian
486 Arctic: True or false? *Clim. Change*, **46**, 485–509, doi:10.1023/A:1005613304674.

487 Førland, E. J., and I. Hanssen-Bauer, 2001: Changes in Temperature and Precipitation in
488 the Norwegian Arctic during the 20th Century. *Detecting and Modelling Regional*
489 *Climate Change*, M.B. India and D.L. Bonillo, Eds., Springer Berlin Heidelberg, Berlin,
490 Heidelberg, 153–161 http://dx.doi.org/10.1007/978-3-662-04313-4_14.

491 Giese, B. S., H. F. Seidel, G. P. Compo, and P. D. Sardeshmukh, 2016: An ensemble of ocean
492 reanalyses for 1815–2013 with sparse observational input. *J. Geophys. Res. Ocean.*,
493 **121**, 6891–6910, doi:10.1002/2016JC012079.

494 Goodison, B. E., P. Y. T. Louie, and D. Yang, 1998: *WMO Solid Precipitation Measurement*
495 *Intercomparison*.

496 Gordon, J. E., V. M. Haynes, and A. Hubbard, 2008: Recent glacier changes and climate

497 trends on South Georgia. *Glob. Planet. Change*, **60**, 72–84,
498 doi:10.1016/j.gloplacha.2006.07.037.

499 Hanssen-Bauer, I., 2002: Temperature and precipitation in Svalbard 1912 – 2050:
500 measurement and scenarios. *Polar Rec. (Gr. Brit.)*, **38**, 225–232.

501 Hogg, O. T., D. K. A. Barnes, and H. J. Griffiths, 2011: Highly diverse, poorly studied and
502 uniquely threatened by climate change: An assessment of marine biodiversity on
503 South Georgia’s continental shelf. *PLoS One*, **6**, doi:10.1371/journal.pone.0019795.

504 Jones, J. M., R. L. Fogt, M. Widmann, G. J. Marshall, P. D. Jones, and M. Visbeck, 2009:
505 Historical SAM variability. Part I: Century-length seasonal reconstructions. *J. Clim.*,
506 **22**, 5319–5345, doi:10.1175/2009JCLI2785.1.

507 —, and Coauthors, 2016a: Assessing recent trends in high-latitude Southern
508 Hemisphere surface climate. *Nat. Clim. Chang.*, **6**, In press,
509 doi:10.1038/nclimate3103. <http://dx.doi.org/10.1038/nclimate3103>.

510 Jones, P. D., C. Harpham, and D. Lister, 2016b: Long-term trends in gale days and
511 storminess for the Falkland Islands. *Int. J. Climatol.*, **36**, 1413–1427,
512 doi:10.1002/joc.4434. <http://doi.wiley.com/10.1002/joc.4434>.

513 Lister, D. H., and P. D. Jones, 2014: Long-term temperature and precipitation records
514 from the Falkland Islands. *Int. J. Climatol.*, **1850**, n/a-n/a, doi:10.1002/joc.4049.
515 <http://doi.wiley.com/10.1002/joc.4049>.

516 Marshall, G. J., 2003: Trends in the Southern Annular Mode from observations and
517 reanalyses. *J. Clim.*, **16**, 4134–4143, doi:10.1175/1520-
518 0442(2003)016<4134:TITSAM>2.0.CO;2.

519 Martin, A. R., and M. G. Richardson, 2017: Rodent eradication scaled up: clearing rats and
520 mice from South Georgia. *Oryx*, 1–9, doi:10.1017/S003060531700028X.
521 <https://www.cambridge.org/core/product/identifier/S003060531700028X/type/>

522 journal_article.

523 Mo, K. C., and R. W. Higgins, 1998: The Pacific–South American Modes and Tropical
524 Convection during the Southern Hemisphere Winter. *Mon. Weather Rev.*, **126**,
525 1581–1596, doi:10.1175/1520-0493(1998)126<1581:TPSAMA>2.0.CO;2.

526 Murphy, E. J., and Coauthors, 2007: Climatically driven fluctuations in Southern Ocean
527 ecosystems. *Proc. R. Soc. B Biol. Sci.*, **274**, 3057–3067, doi:10.1098/rspb.2007.1180.
528 <http://rspb.royalsocietypublishing.org/cgi/doi/10.1098/rspb.2007.1180>.

529 van Oldenborgh, G. J., and G. Burgers, 2005: Searching for decadal variations in ENSO
530 precipitation teleconnections. *Geophys. Res. Lett.*, **32**, 1–5,
531 doi:10.1029/2005GL023110.

532 Richard, Y., and Coauthors, 2013: Temperature changes in the mid- and high- latitudes
533 of the Southern Hemisphere. *Int. J. Climatol.*, **33**, 1948–1963, doi:10.1002/joc.3563.
534 <http://doi.wiley.com/10.1002/joc.3563>.

535 Sardeshmukh, P. D., G. P. Compo, and C. Penland, 2015: Need for caution in interpreting
536 extreme weather statistics. *J. Clim.*, **28**, 9166–9187, doi:10.1175/JCLI-D-15-0020.1.

537 Skansi, M., and Coauthors, 2017: Evaluating Highest-Temperature Extremes in the
538 Antarctic. *Eos (Washington, DC)*, 1–6, doi:10.1029/2017EO068325.
539 [https://eos.org/features/evaluating-highest-temperature-extremes-in-the-](https://eos.org/features/evaluating-highest-temperature-extremes-in-the-antarctic)
540 antarctic.

541 Thomas, E. R., G. J. Marshall, and J. R. McConnell, 2008: A doubling in snow accumulation
542 in the western Antarctic Peninsula since 1850. *Geophys. Res. Lett.*, **35**, 1–5,
543 doi:10.1029/2007GL032529.

544 Thompson, D. W. J., and S. Solomon, 2002: Interpretation of Recent Southern
545 Hemisphere Climate Change. *Science (80-.)*, **296**, 895–899,
546 doi:10.1126/science.1087440.

547 <http://www.sciencemag.org/cgi/content/abstract/302/5643/273>.

548 Thompson, D. W. J., S. Solomon, P. J. Kushner, M. H. England, K. M. Grise, and D. J. Karoly,
549 2011: Signatures of the Antarctic ozone hole in Southern Hemisphere surface
550 climate change. *Nat. Geosci.*, **4**, 741–749, doi:10.1038/ngeo1296.
551 <http://dx.doi.org/10.1038/ngeo1296>.

552 Trathan, P. N., J. Forcada, and E. J. Murphy, 2012: Environmental Forcing and Southern
553 Ocean Marine Predator Populations: Effects of Climate Change and Variability.
554 *Antarctic Ecosystems: An Extreme Environment in a Changing World*, John Wiley &
555 Sons, Ltd, Chichester, UK.

556 Turner, J., and Coauthors, 2005: Antarctic climate change during the last 50 years. *Int. J.*
557 *Climatol.*, **25**, 279–294, doi:10.1002/joc.1130.

558 Turney, C. S. M., and Coauthors, 2016a: Anomalous mid-twentieth century atmospheric
559 circulation change over the South Atlantic compared to the last 6000 years. *Environ.*
560 *Res. Lett.*, **11**, 64009, doi:10.1088/1748-9326/11/6/064009.
561 <http://dx.doi.org/10.1088/1748-9326/11/6/064009>.

562 Turney, C. S. M., and Coauthors, 2016b: Anomalous mid-twentieth century atmospheric
563 circulation change over the South Atlantic compared to the last 6000 years. *Environ.*
564 *Res. Lett.*, doi:10.1088/1748-9326/11/6/064009.
565 [http://www.scopus.com/inward/record.url?eid=2-s2.0-](http://www.scopus.com/inward/record.url?eid=2-s2.0-84977547766&partnerID=MN8TOARS)
566 [84977547766&partnerID=MN8TOARS](http://www.scopus.com/inward/record.url?eid=2-s2.0-84977547766&partnerID=MN8TOARS).

567 Turney, C. S. M., and Coauthors, 2017: Tropical forcing of increased Southern Ocean
568 climate variability revealed by a 140-year subantarctic temperature reconstruction.
569 *Clim. Past*, doi:10.5194/cp-13-231-2017.

570 Visbeck, M., 2009: A station-based southern annular mode index from 1884 to 2005. *J.*
571 *Clim.*, **22**, 940–950, doi:10.1175/2008JCLI2260.1.

572 Wang, X. L., 2008a: Accounting for autocorrelation in detecting mean shifts in climate
573 data series using the penalized maximal t or F test. *J. Appl. Meteorol. Climatol.*, **47**,
574 2423–2444, doi:10.1175/2008JAMC1741.1.

575 ———, 2008b: Penalized maximal F test for detecting undocumented mean shift without
576 trend change. *J. Atmos. Ocean. Technol.*, **25**, 368–384,
577 doi:10.1175/2007JTECHA982.1.

578 Wang, X. L., and Y. Feng, 2013: RHtestsV4 User Manual.

579 Whitehouse, M. J., M. P. Meredith, P. Rothery, A. Atkinson, P. Ward, and R. E. Korb, 2008:
580 Rapid warming of the ocean around South Georgia, Southern Ocean, during the 20th
581 century: Forcings, characteristics and implications for lower trophic levels. *Deep.*
582 *Res. Part I Oceanogr. Res. Pap.*, **55**, 1218–1228, doi:10.1016/j.dsr.2008.06.002.

583 Zazulie, N., M. Rusticucci, and S. Solomon, 2010: Changes in climate at high southern
584 latitudes: A unique daily record at Orcadas spanning 1903-2008. *J. Clim.*, **23**, 189–
585 196, doi:10.1175/2009JCLI3074.1.

586 Zhang, X., L. Alexander, G. C. Hegerl, P. Jones, A. K. Tank, T. C. Peterson, B. Trewin, and F.
587 W. Zwiers, 2011: Indices for monitoring changes in extremes based on daily
588 temperature and precipitation data. *Wiley Interdiscip. Rev. Clim. Chang.*, **2**, 851–870,
589 doi:10.1002/wcc.147.

590

591 **Tables**

	1907-1950	1950-2016	1950-1983	1907-2016
South Georgia Observations				
TM Annual	-0.097	0.11***	0.14	0.13***
Std. err.	0.0107	0.0037	0.0090	0.0026
p value	0.370	0.0043	0.143	8.36E-06
TM SON	-0.14	0.14**	0.19	0.14***
Std. err.	0.0134	0.005	0.015	0.0034

<i>p</i> value	0.291	0.012	0.221	9.32E-05
TM DJF	-0.01	0.22***	0.31**	0.16***
Std. err.	0.014	0.006	0.014	0.003
<i>p</i> value	0.970	0.001	0.030	1.14E-05
TM MAM	-0.09	0.03	-0.07	0.08**
Std. err.	0.0133	0.0063	0.0165	0.0032
<i>p</i> value	0.506	0.703	0.684	0.0159
TM JJA	0.13	0.09*	0.06	0.16***
Std. err.	0.014	0.005	0.014	0.003
<i>p</i> value	0.370	0.068	0.660	1.85E-06
Twentieth Century Reanalysis:20CR v2c				
TM Annual	0.01***	0.04**	0.21***	0.08***
Std. err.	0.952	0.123	0.0001	0.0017
<i>p</i> value	0.009	0.003	0.004	1.31E-05

592

593 **Table 1:** Trends (°C per decade) for mean monthly mean temperature and seasons, with
594 standard error, and *p*-values for selected periods of time (** where $p < 0.01$; ** where
595 $p < 0.05$; * where $p < 0.1$) for observations at South Georgia, and the Twentieth Century
596 Reanalysis.

597

598

	1907-1950	1907-1983	1950-1983	1907-2016
TM Annual	18.8	43.8***	94.4*	45.1***
Std. err.	4.144	1.583	5.316	1.426
<i>p</i> value	0.654	0.008	0.089	0.003
TM SON	9.14	16.8***	30.3	15.7***
Std. err.	1.247	0.542	2.215	0.422
<i>p</i> value	0.468	0.002	0.183	0.0004
TM DJF	12.3	13.0**	-7.80	10.3**
Std. err.	1.648	0.590	1.948	0.494
<i>p</i> value	0.459	0.031	0.692	0.041
TM MAM	-9.11	10.9*	15.6	15.2***
Std. err.	1.460	0.621	2.497	0.487
<i>p</i> value	0.537	0.082	0.538	0.003
TM JJA	17.8	9.60	48.3**	15.3**

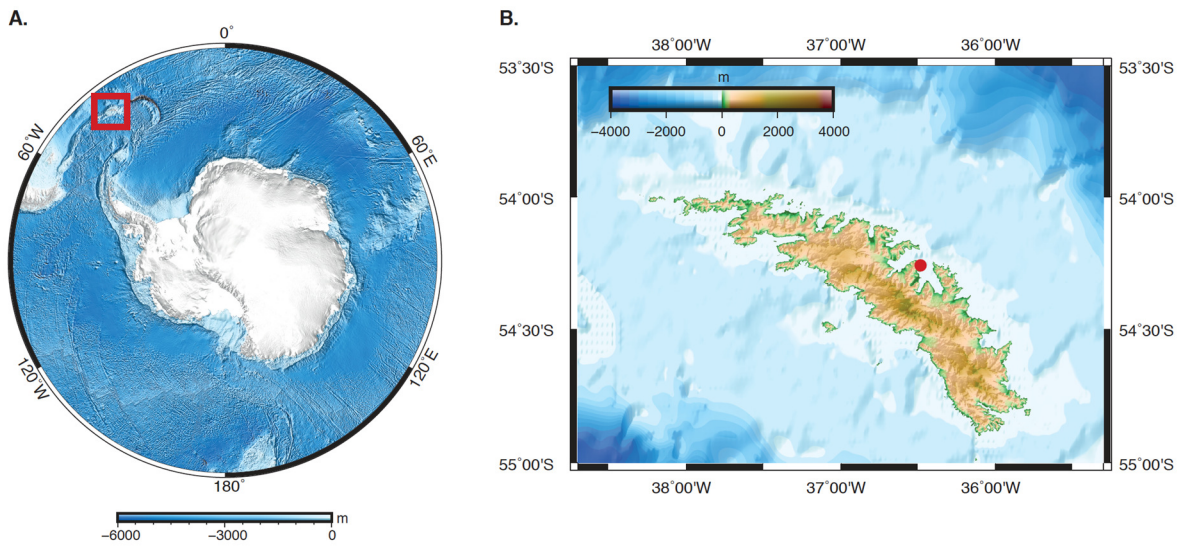
Std. err.	2.119	0.745	1.824	0.611
p value	0.406	0.202	0.014	0.014

599

600 **Table 2:** Trends (precipitation sum (mm) per decade) for mean monthly precipitation sum,
601 with standard error, and p-values for selected periods of time (** where $p < 0.01$; * where
602 $p < 0.05$; * where $p < 0.1$).

603

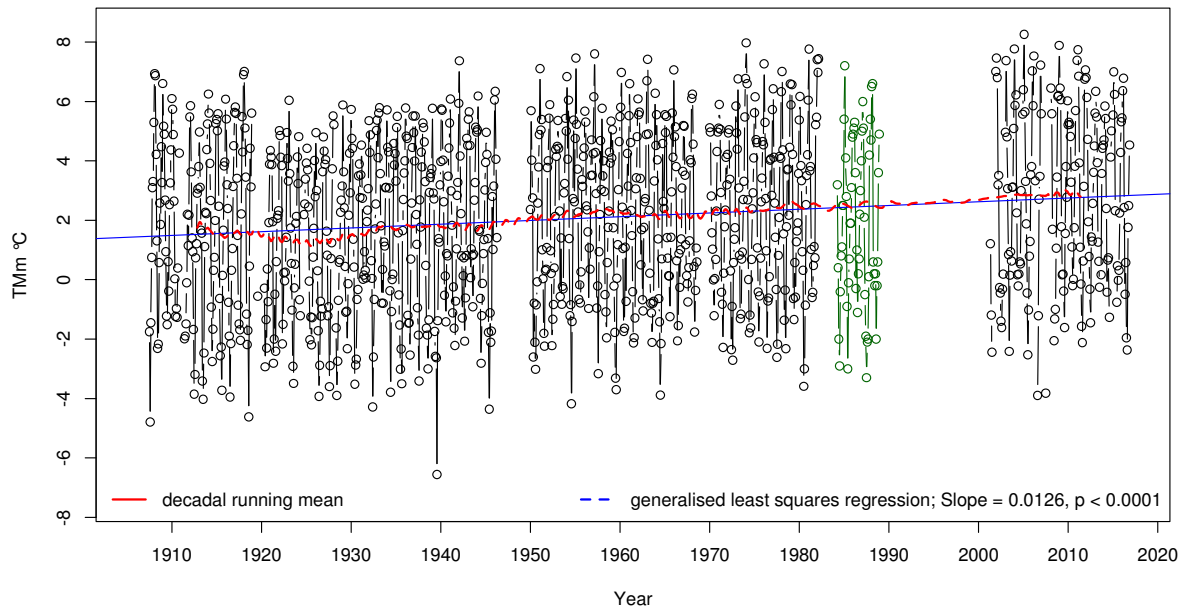
604 **Figures**



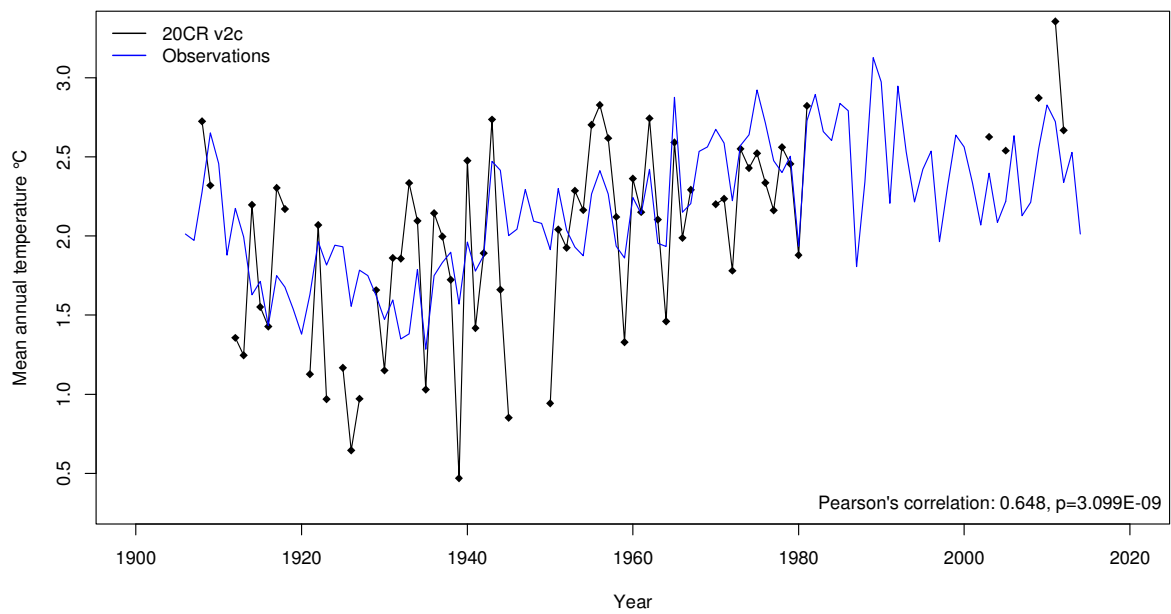
605

606 **Figure 1** Location of South Georgia (red square, Panel A), and the meteorological station
607 at Grytviken in Cumberland Bay (red dot, Panel B).

608



609

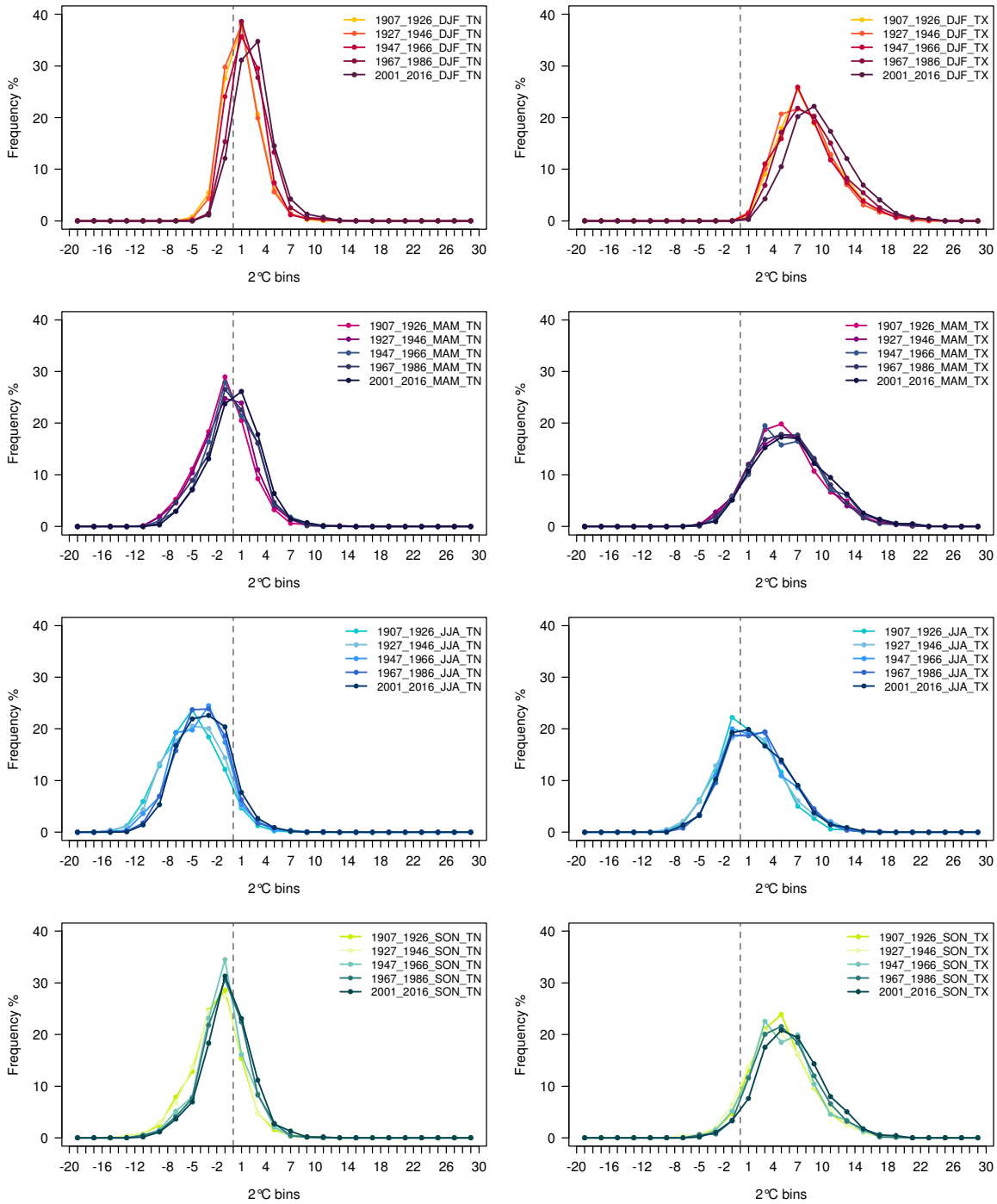


610

611 **Figure 2 A.** Average mean monthly temperature from South Georgia, with generalised
 612 least squares regression (blue) and decadal running mean (red) lines shown. Dark green
 613 data (1984-1988) from military station is unverified and not included in the linear
 614 regression or decadal running mean. **B.** Mean annual air temperature from the Twentieth

615 Century Reanalysis (20CR v2c) plotted against South Georgia mean annual temperature
616 from observations.

617

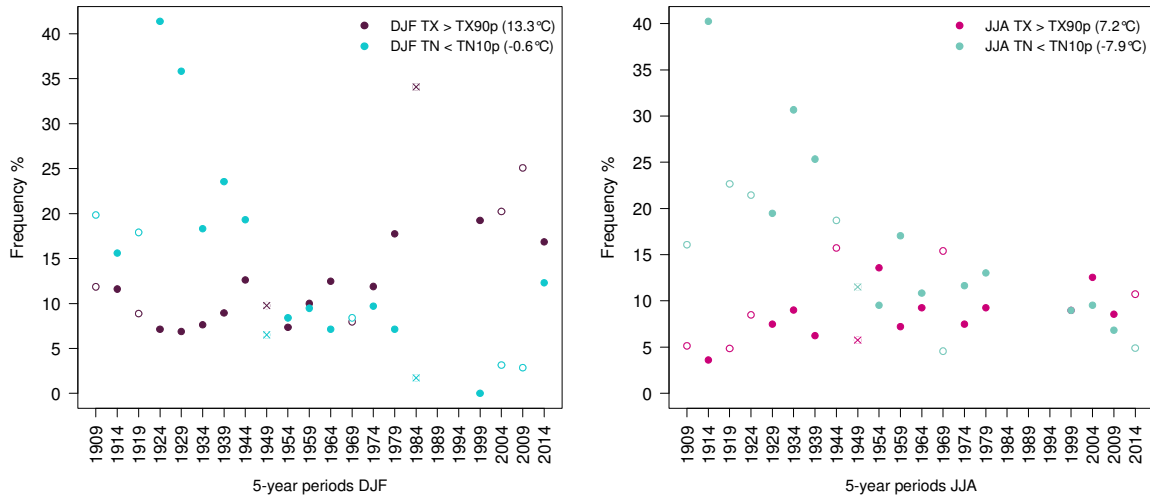


618

619 **Figure 3** Distribution of frequencies of daily minimum (TN; left column) and maximum
620 (TX; right column) temperatures during December-February (DJF), March-May (MAM),

621 *June-August (JJA) and September-November (SON) for 20-year periods since 1907. Note*
 622 *data gap between 1983-2001. Dashed line at 0°C. Two degree bins have been used.*

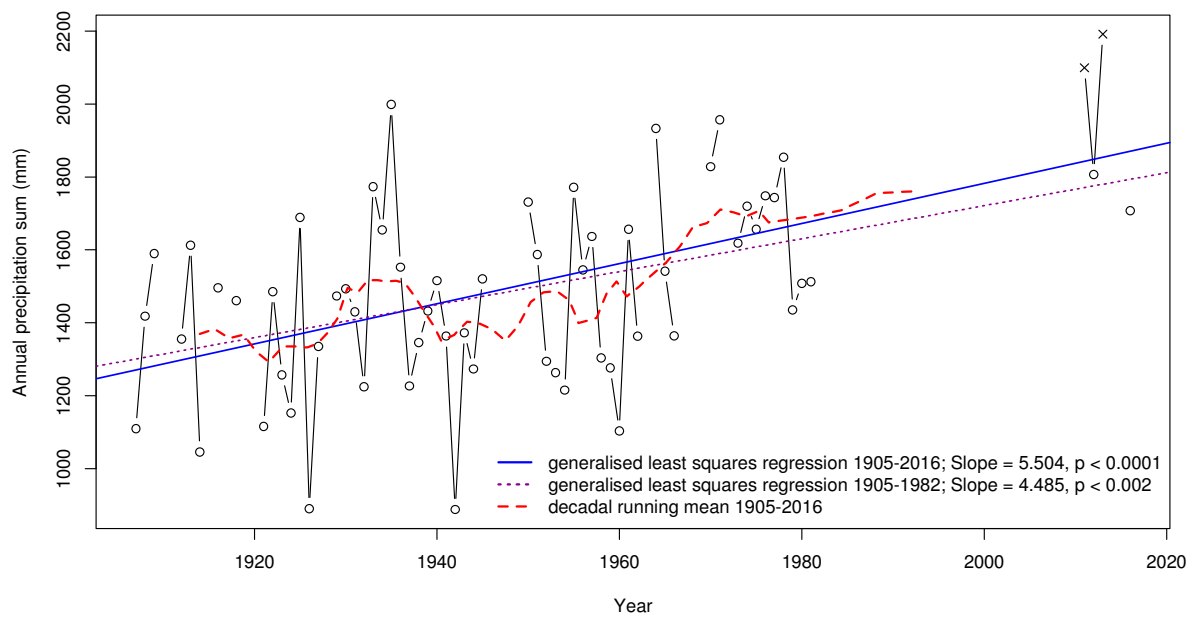
623



624

625 **Figure 4** *Changes in the percentages of relatively warm days (TX90p; purple) and cold*
 626 *days (TN10p; blue) for 5-year periods for December-February (DJF), and for relatively*
 627 *warm days (TX90p; pink) and cold days (TN10p; green) for 5-year periods for June-August*
 628 *(JJA). Open circles indicate periods where only 3 or 4 years of data were available; crosses*
 629 *where 1 or 2 years of data were available.*

630

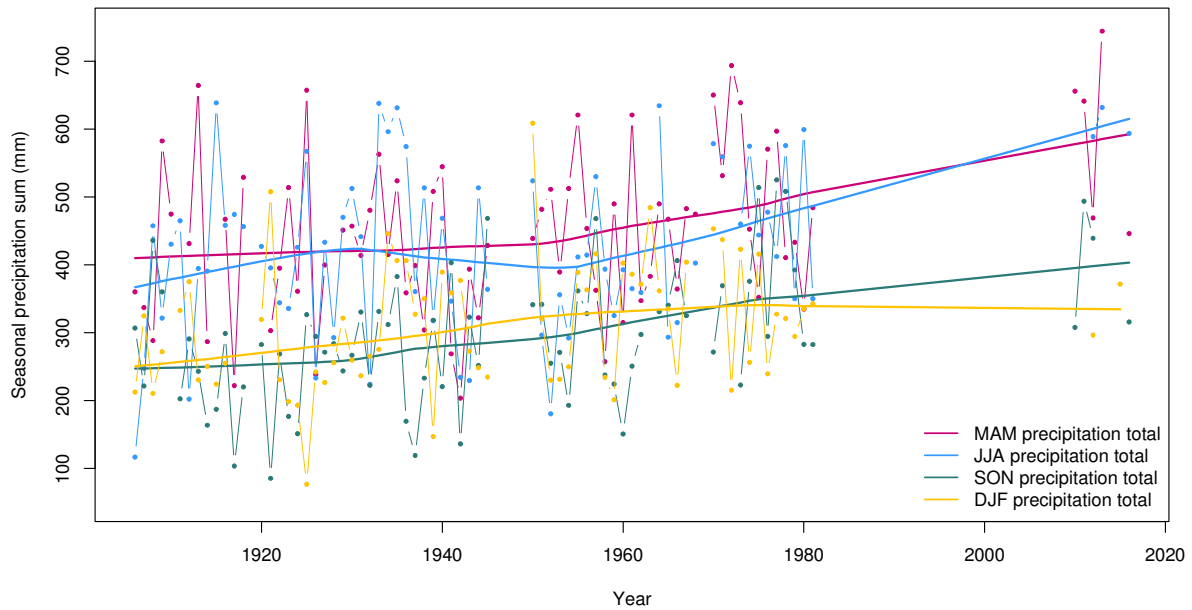


631

632 **Figure 5** Annual precipitation totals (in mm), including only years with no missing
 633 observations (open circles), and years with <6 missing days per year (crosses), with linear
 634 regressions for the years 1905-1982 and 1905-2016, and a decadal running mean (1905-
 635 2016).

636

637

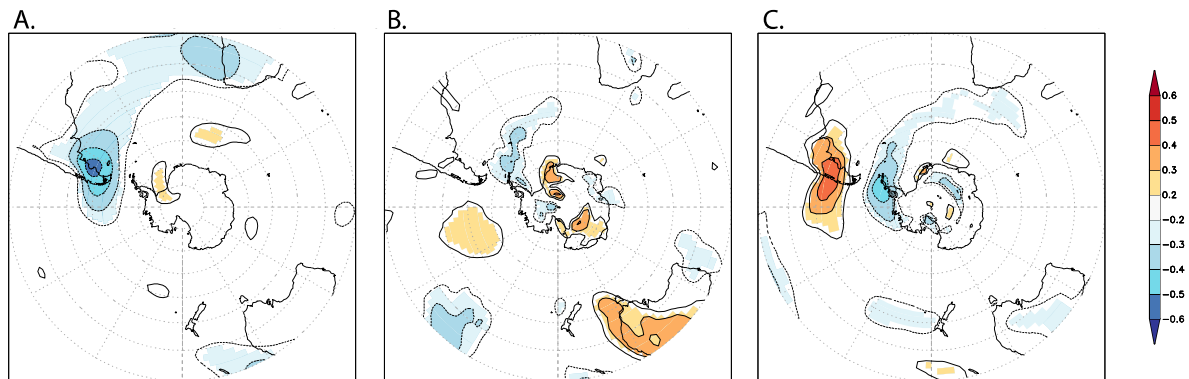


638

639 **Figure 6** Seasonal precipitation totals, including only years with <3 missing days per
 640 season, each with a locally weighted scatterplot smoothing (1905-2016).

641

642

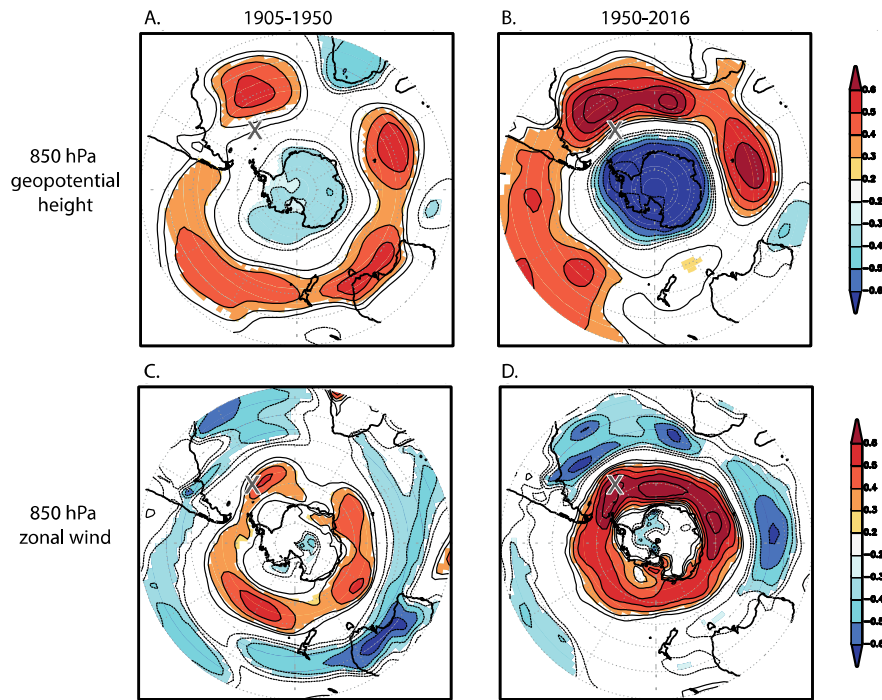


643

644 **Figure 7** Correlations between the detrended and deseasonalised monthly precipitation
 645 sum from South Georgia (marked with an 'X') and A. 850 hPa geopotential height, B. 850
 646 hPa meridional, C. 850 hPa zonal, averaged over March to August over the period 1905-
 647 1983 using the Twentieth Century Reanalysis (20CR) version 2c. Significance $p_{field} < 0.1$.
 648 Analyses were made with KNMI Climate Explorer (van Oldenborgh and Burgers 2005).

649

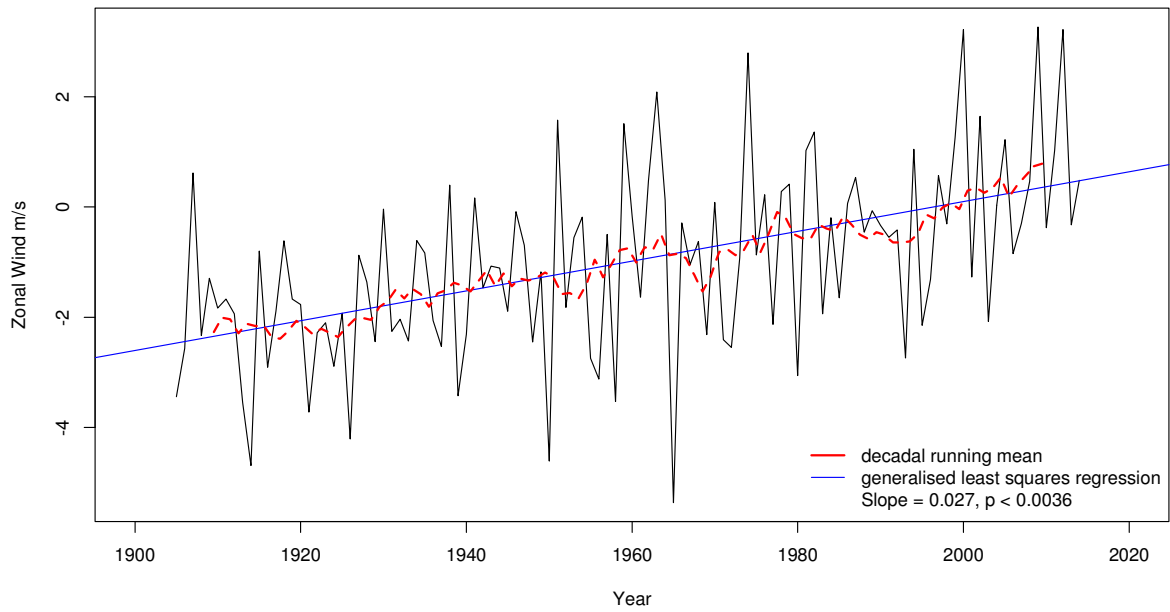
650



651

652 **Figure 8** Correlations between the detrended and deseasonalised mean monthly
653 temperature from South Georgia (marked with an 'X') and A. 850 hPa geopotential height
654 (1905-1950), B. 850 hPa geopotential height (1950-2016), C. 850 hPa zonal wind (1905-
655 1950), and D. 850 hPa zonal wind (1950-2016), averaged over December to February
656 using the Twentieth Century Reanalysis (20CR) version 2c. Significance $p_{field} < 0.1$. Analyses
657 were made with KNMI Climate Explorer (van Oldenborgh and Burgers 2005).

658



659

660 **Figure 9** Zonal wind speed at 850 hPa from the 20th Century Reanalysis (20CR v2c)
 661 averaged over December-February at South Georgia, with generalised least squares
 662 regression (blue) and decadal running mean (red) lines shown.

663